Publisher

www.singhpublication.com

E-ISSN:2583-2468

Applied Science and Engineering Journal for Advanced Research

2025 Volume 4 Number 2 March

Research Article

Linear Motor

Design of a Trajectory Tracking Controller for Coreless Tubular Linear Motor Using Model Predictive Controller

Nguyen Trung Thanh[1*], Nguyen Minh Cuong[2], Dang Danh Hoang[3], Le Thi Thuy Ngan[4]

DOI:10.5281/zenodo.15104520

[1*] Nguyen Trung Thanh, Faculty of Mechanical, Electrical, Electronics Technology, Thai Nguyen University of Technology, Vietnam.

[2] Nguyen Minh Cuong, Faculty of Electrical Engineering, Thai Nguyen University of Technology, Vietnam.

[3] Dang Danh Hoang, Faculty of Mechanical, Electrical, Electronics Technology, Thai Nguyen University of Technology, Vietnam.

[4] Le Thi Thuy Ngan, Faculty of Mechanical, Electrical, Electronics Technology, Thai Nguyen University of Technology, Vietnam.

This paper presents a cascaded control structure for a coreless tubular linear motor. The system includes position and speed loops employing PI controllers, and a current loop using Finite Control Set Model Predictive Control (FCS-MPC). This structure addresses challenges associated with low stator inductance, specifically its impact on current control. A simulation model was developed using MATLAB/Simulink. The simulation results demonstrate the effectiveness of the proposed solution in tracking the desired trajectory and minimizing the negative effects of low stator inductance on the current loop.

Keywords: fcs-mpc, tubular linear motor, coreless linear motor

Corresponding Author

Nguyen Trung Thanh, Faculty of Mechanical, Electrical, Electronics Technology, Thai Nguyen University of Technology, Vietnam.

Email: nguyentrungthanh@tnut.edu.vn

How to Cite this Article

Nguyen Trung Thanh, Nguyen Minh Cuong, Dang Danh Hoang, Le Thi Thuy Ngan, Design of a Trajectory Tracking Controller for Coreless Tubular Linear Motor Using Model Predictive Controller. Appl. Sci. Eng. J. Adv. Res.. 2025;4(2):1-7.

Available From

https://asejar.singhpublication.com/index.php/ojs/article/view/131

To Browse

Manuscript Received	Review Round 1	Review Round 2	Review Round 3	Accepted
2025-02-03	2025-02-24			2025-03-17
Conflict of Interest	**Funding**	**Ethical Approval**	**Plagiarism X-checker**	**Note**
None	Nil	Yes	3.44	

1. Introduction

The applications of linear motors are becoming increasingly widespread in both industrial and domestic settings. These applications include industrial automation, transportation, renewable energy, and more[1-3]. The advantage of linear motors lies in their ability to provide direct thrust without the need for complex mechanical structures [4-6]. As a result, they are highly suitable for applications requiring high reliability, high efficiency, and compact dimensions. There are various types of linear motor based on their configurations. These configurations include flat single-sided, flat double-sided, and tubular structures [7, 8]. However, they share a common feature: the stator windings surround the rotor, which is composed of permanent magnets. In the tubular structure, the stator consists of disk-shaped coils arranged coaxially, while the rotor is formed by cylindrical magnets sequentially placed within a circular tubular housing (Figure 1).

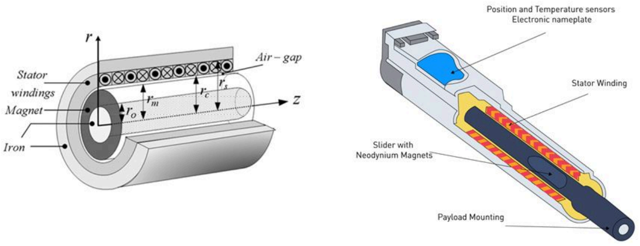

Figure 1: Structure of a Tubular Linear Motor [8]

Tubular linear motors can be constructed with or without an iron core [9, 10]. However, tubular linear motors are predominantly manufactured without an iron core. The absence of an iron core in the stator results in low stator inductance and causes thrust force ripple [11]. Although PID controllers are effectively applied to rotary motors [12, 13], raditional methods still have limitations, such as not considering control signal constraints, state constraints, the impact of load disturbances, and variations in system inertia[14]. For coreless tubular linear motors, the rotor shaft is more sensitive to load disturbances due to the lack of intermediate transmission mechanisms. PID controllers also often produce large, undesirable overshoots. The current loop is the primary cause of this problem. To address these issues, modern controllers have been applied, such as sliding mode controllers [15, 16], fuzzy controllers [17, 18], and adaptive controllers using neural networks [19-21]. However, these solutions often overlook the limitations of the power converter. Meanwhile, the power converter has only a limited ability to provide energy responses.

A control structure is proposed, employing PI controllers for the speed and position loops and Finite Control Set Model Predictive Control (FCS-MPC) for the current loop. The design of these controllers, considering input constraints, is presented in Section 2. A simulation in MATLAB/Simulink is then used to evaluate the performance of the proposed solution.

2. Control Design

a. Discretized Model of the Coreless Tubular Linear Motor

The mathematical model of the tubular linear motor is described based on the principles of electromagnetism. Based on this, an approach to modeling the mathematical system in the dq coordinate frame is established, as presented in reference[22].

$$\begin{cases} \frac{di_d}{dt} = \frac{u_d}{L_s} - \frac{R_s}{L_s} i_d + w_r i_q \\ \frac{di_q}{dt} = \frac{u_q}{L_s} - \frac{R_s}{L_s} i_q - w_r i_d - \frac{w_r}{L_s} y_f \end{cases} \tag{1}$$

Where: i_d and i_q are the currents on the d-axis and q-axis, respectively; u_d and u_q are the output voltages of the converter on the d-axis and q-axis, respectively. is the magnetic flux generated by the permanent magnets of the rotor; ω_r is the angular velocity converted from the linear velocity of the motor and is determined by the following expression:

$w_r = \frac{p}{t} v$ where v is the linear velocity of the rotor.

And the thrust force is determined by the expression:

$$F_T = \frac{3}{2} \frac{pp}{t} k_F \left(y_d i_q - y_q i_d \right) \tag{2}$$

where p is the number of pole pairs of the motor, y_d y_q are the magnetic fluxes generated by the permanent magnets on the d-axis and q-axis, respectively.

To facilitate the design of the controller, we choose the d-axis to align with the magnetic flux axis of the rotor's permanent magnets. Therefore, the thrust force expression can be rewritten as follows:

$$F_T = \frac{3}{2}\frac{pp}{t} k_F y_f i_q \tag{3}$$

Applying Newton's second law to the motor, we obtain the dynamic equation of the motor:

$$\begin{cases} \dfrac{dx}{dt} = v \\ \dfrac{dv}{dt} = \dfrac{1}{m}\left(F_T - F_L\right) \end{cases} \tag{4}$$

From Error! Reference source not found., Error! Reference source not found. and Error! Reference source not found., the motor model can be rewritten in matrix form as:

$$\frac{d\mathbf{i}_{dq}}{dt} = \mathbf{T}\mathbf{i}_{dq} + \mathbf{L}\mathbf{u}_{dq} + \mathbf{W}\mathbf{i}_{qd} w_r + \mathbf{P} y_f w_r \tag{5}$$

where

$$\mathbf{i}_{dq} = \begin{bmatrix} i_d & i_q \end{bmatrix}^T;\ \mathbf{i}_{qd} = \begin{bmatrix} i_q & i_d \end{bmatrix}^T;\ \mathbf{T} = \begin{bmatrix} \dfrac{R_s}{L_s} \end{bmatrix};\ \mathbf{L} = \begin{bmatrix} \dfrac{1}{L_s} \end{bmatrix};\ \mathbf{W} = \begin{bmatrix} 0 & 1 \\ 1 & 0 \end{bmatrix};\ \mathbf{P} = \begin{bmatrix} 0 \\ 1/L_s \end{bmatrix}$$

Equations Error! Reference source not found. and Error! Reference source not found. form the basis for designing the position, speed, and current controllers in the following section.

b. Outer-Loop Controller Design

Based on the system of equations Error! Reference source not found., a cascaded two-loop control structure is designed. The equations presented in Error! Reference source not found. can be expressed in the following transfer function form:

$$\begin{cases} G_x(s) = \dfrac{X(s)}{V(s)} = \dfrac{1}{s} \\ G_v(s) = \dfrac{V(s)}{I_q(s)} = \dfrac{3}{2} k_F y_f \dfrac{pp}{t\,m}\dfrac{1}{s} \end{cases} \tag{6}$$

The plant for each controller is considered to be an integrator; therefore, a PI controller can be chosen with the following form:

$$u(s) = K_p\left(1 + \frac{1}{T_i s}\right)e(s) \tag{7}$$

Applying the pole placement method with the desired specifications, the controller parameters for the position loop and speed loop are obtained.

c. Inter-Loop Controller Design

To design the current controller, the motor description equation Error! Reference source not found. is discretized with a sampling time Ts as follows:

$$\mathbf{i}_{dq}(k+1) = \mathbf{i}_{dq}(k) + \mathbf{T}_s\mathbf{i}_{dq}(k) + \mathbf{L}_s\mathbf{u}_{dq}(k) + \mathbf{W}_s\mathbf{i}_{qd}(k)w_r(k) + \mathbf{P}_s y_f w_r(k) \tag{8}$$

where

$$\mathbf{T}_s = T_s\begin{bmatrix} \dfrac{R_s}{L_s} \end{bmatrix};\ \mathbf{L}_s = T_s\begin{bmatrix} \dfrac{1}{L_s} \end{bmatrix};\ \mathbf{W}_s = T_s\begin{bmatrix} 0 & 1 \\ 1 & 0 \end{bmatrix};\ \mathbf{P}_s = T_s\begin{bmatrix} 0 \\ 1/L_s \end{bmatrix}$$

With Ts being the sampling time of the current, typically equal to the carrier frequency of the converter, from the discretized model Error! Reference source not found., we can rewrite it as follows:

$$\begin{aligned} \mathbf{i}_{dq}(k+1) &= \mathbf{i}_{dq}(k) + \mathbf{T}_s\mathbf{i}_{dq}(k) + \mathbf{W}_s\mathbf{i}_{qd}(k)w_r(k) + \mathbf{L}_s\mathbf{u}_{dq}(k) + \mathbf{P}_s y_f w_r(k) \\ &= \mathbf{\Phi}\mathbf{i}_{dq}(k) + \mathbf{L}_s\mathbf{u}_{dq}(k) + \mathbf{P}_s y_f w_r(k) \end{aligned} \tag{9}$$

where $\mathbf{\Phi} = T_s\left[\mathbf{I} + \mathbf{T}_s + \mathbf{W}_s w_r(k)\right]$

Based on the discretized model Error! Reference source not found., a current prediction model is constructed as follows:

$$\mathbf{i}^{est}_{dq}(k+i+1 \mid k) = \mathbf{\Phi}\mathbf{i}^{est}_{dq}(k+i \mid k) + \mathbf{L}_s\bar{\mathbf{u}}_{dq}(k) + \mathbf{P}_s y_f w_r(k) \tag{10}$$

Where $\mathbf{i}^{est}_{dq}(k) = \mathbf{i}_{dq}(k)$ is the current at the k-th sampling time; is the control signal for the next i-th step, with the prediction horizon N. The goal of the controller is to find an optimal control value. We select the value function in the following quadratic form:

$$J = \sum_{i=1}^{N}\left\{\left(\mathbf{i}^{ref}_{dq} - \mathbf{i}^{est}_{dq}(k+i)\right)\mathbf{Q}\left(\mathbf{i}^{ref}_{dq} - \mathbf{i}^{est}_{dq}(k+i)\right)\right\} \tag{11}$$

Where $\mathbf{Q} = \begin{bmatrix} & 0 \\ & 1 \end{bmatrix}$ is a positive definite diagonal matrix, the coefficient *ld* is the weighting factor of the deviation in the value function J. $\mathbf{i}^{ref}_{dq}$ is the output of the outer-loop controller.

The control signal udq is generated by a three-phase inverter. This converter uses the SVM modulation method based on 6 basic vectors. With this method, the modulation values are normalized to form the vector $\mathbf{u}_s = \begin{bmatrix} u_a & u_b & u_c \end{bmatrix}^T$. Therefore, a finite number of voltage vectors can be applied to the motor. In this paper, six fundamental vectors and six vectors created by pulse-width modulating the fundamental vectors to half their magnitude are used to form the vector set $\mathbf{U} = \left\{\mathbf{u}_0, \mathbf{T}\mathbf{u}_1, \mathbf{T}\mathbf{u}_2, \ldots, \mathbf{T}\mathbf{u}_{11}, \mathbf{T}\mathbf{u}_{12}\right\}$, as shown in Fig. 3.

The minimization of can be achieved by sequentially replacing each voltage vector in Table 1 to find the optimal control signal. This approach helps reduce the computation time of the system, enabling a quick response to changes in load disturbances.

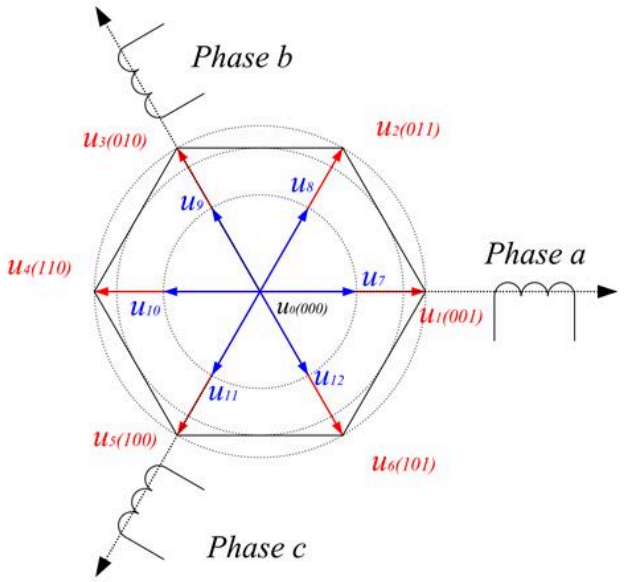

Figure 2: The voltage vectors **U**

To reduce the computation time, the prediction horizon is limited to N=2. Substituting equation into equation Error! Reference source not found., the condition for the control signal u_{dq} is obtained as follows:

$$\begin{aligned}\min_{\bar{\mathbf{u}}_{dq}(k),\bar{\mathbf{u}}_{dq}(k+1)} J &= \bar{\mathbf{u}}_{dq}^T(k)\mathbf{H}^T\mathbf{Q}\mathbf{H}\bar{\mathbf{u}}_{dq}(k) + \bar{\mathbf{u}}_{dq}^T(k+1)\mathbf{H}^T\mathbf{Q}\mathbf{H}\bar{\mathbf{u}}_{dq}(k+1) \\ &+ \bar{\mathbf{u}}_{dq}^T(k)\mathbf{H}^T\mathbf{Q}^T\mathbf{Q}\mathbf{H}\bar{\mathbf{u}}_{dq}(k+1) + 2\left(\mathbf{\Phi}\mathbf{i}_{dq}(k) + \mathbf{h}y_f - \mathbf{i}_{dq}^{ref}\right)^T\mathbf{Q}\mathbf{H}\bar{\mathbf{u}}_{dq}(k) \\ &+ 2\left(\mathbf{\Phi}^2\mathbf{i}_{dq}(k) + \mathbf{\Phi}\mathbf{h}y_f - \mathbf{i}_{dq}^{ref}\right)^T\mathbf{Q}\mathbf{H}\bar{\mathbf{u}}_{dq}(k+1)\end{aligned} \tag{12}$$

With $\bar{\mathbf{u}}_{dq} \in \mathbf{U} = \{\mathbf{u}_0, \mathbf{T}\mathbf{u}_1, \mathbf{T}\mathbf{u}_2, ..., \mathbf{T}\mathbf{u}_{11}, \mathbf{T}\mathbf{u}_{12}\}$

where $\mathbf{T} = \begin{bmatrix} \cos(\theta) & -\sin(\theta) \\ \cos(\theta - 2\pi/3) & -\sin(\theta - 2\pi/3) \\ \cos(\theta + 2\pi/3) & -\sin(\theta + 2\pi/3) \end{bmatrix}$

Expression represents the condition for determining the control signal u_{dq} for the current loop. By applying minimization algorithms to solve the system of equations Error! Reference source not found., we obtain the desired optimal control signal.

3. Simulation Results

To validate the controllers obtained by minimizing the objective functions in Error! Reference source not found., a simulation model was developed using Matlab/Simulink software, with the motor parameters provided in Table 1.

Table 1: Motor parameters

Motor parameters	Symbol	Value	Unit
d-axis stator inductance	L_{sd}	1.4	mH
q-axis stator inductance	L_{sq}	1.4	mH
Stator resistance	R_s	10.3	Ω
Rotor flux	ψ_p	0.035	Wb
Number of pole pairs	z_p	2	
Pole step	τ_p	0.02	m

A simulation scenario was designed to test the response capability of the entire system. A straight-line trajectory was used for this purpose. To ensure the differentiability of the trajectory, the set speed was kept constant during the motor's movement. Specifically, the motor moves from the position 0mm to 80mm in 0.5s with a speed of 160mm/s and maintains the position for 1s. After that, the motor moves back to the 0mm position in 0.5s with a speed of 160mm/s. At t=1s, a load force F_L=5N is applied.

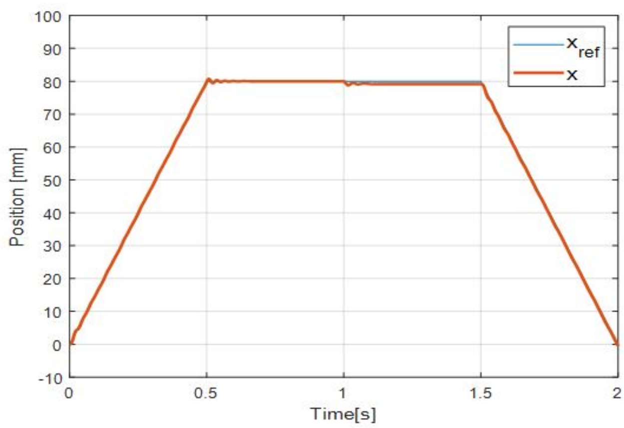

Figure 3: The position response of the motor

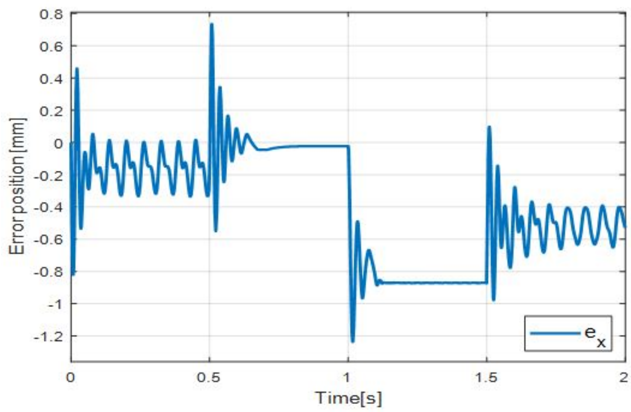

Figure 4: The error position of the motor

The trajectory and response of the motor are shown in Figure 3, demonstrating the ability to track the reference trajectory.

The position error of the motor relative to the trajectory, with e_{xmax}=0.8mm, meets the specified quality criteria.

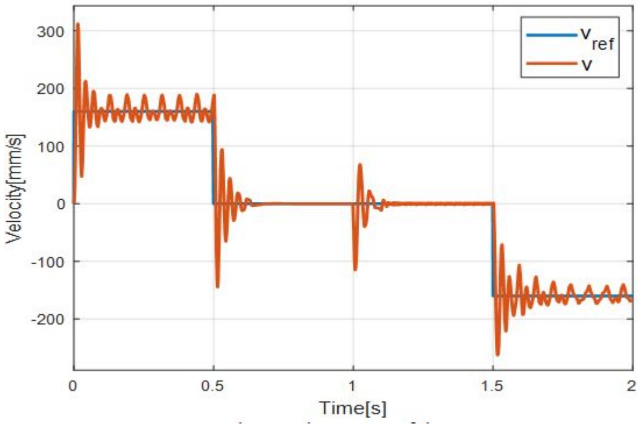

Figure 5: The speed response of the motor

Meanwhile, the motor speed tracks the set speed during the motor's movement. However, the speed fluctuations during the movement are caused by the limited number of current vectors used in the inner-loop controller, as shown in Figures 5.

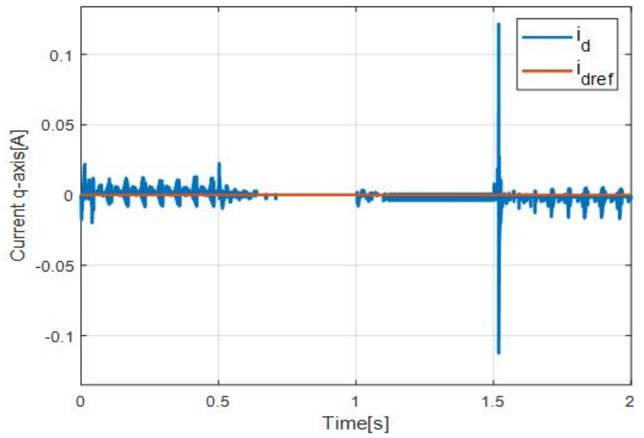

Figure 6: Response of current id

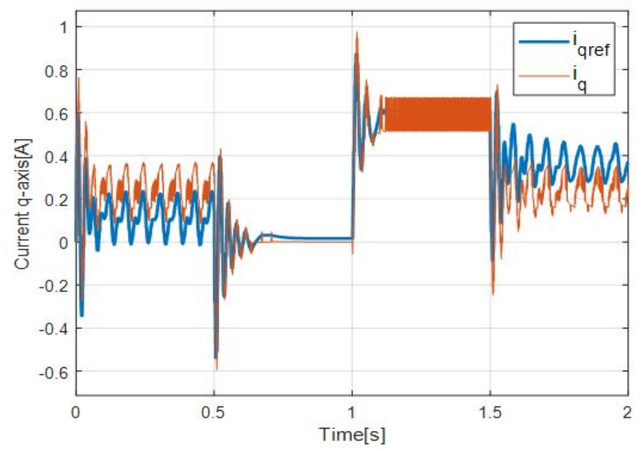

Figure 7: Response of current iq

In order to reduce the computational load, the prediction horizon and the number of voltage vectors used are limited. In the simulation results with a prediction horizon of N = 2 and the number of voltage vectors used n = 13, the results in Figures 6 and 7 demonstrate the rapid response capability of the current controller to changes in the reference value.

4. Conclusion

This paper presents a proposed control structure with two control loops: the speed and position loop, and the current loop. In this structure, the outer loop is designed using a PI controller to stability position and velocity. Meanwhile, the inner loop (current loop) is designed using the FCS-MPC controller to respond quickly to changes in the current under low stator inductance conditions. The simulation results demonstrate that the combination of the two loops significantly improves the overall system response. In particular, it overcomes the fundamental drawback of traditional PID controllers.

Acknowledgment

The authors gratefully acknowledge Thai Nguyen University of Technology, Vietnam, for supporting this work.

References

1. Wakiwaka, H. (2024). Magnetic application in linear motor. in *Handbook of Magnetic Material for Motor Drive Systems,* pp. 1-16. Singapore: Springer Nature Singapore. https://doi.org/10.1007/978-981-19-9644-3_54-1.

2. Gang, L. Y. U. (2020). Review of the application and key technology in the linear motor for the rail transit. *Proceedings of the CSEE*, *40*(17), 5665-5675. doi:10.13334/j.0258-8013.pcsee.200488.

3. Jansen, J. W., Smeets, J. P. C., Overboom, T. T., Rovers, J. M. M., & Lomonova, E. A. (2014). Overview of analytical models for the design of linear and planar motors. *IEEE Transactions on Magnetics*, *50*(11), 1-7. doi:10.1109/TMAG.2014.2328556.

4. Boldea, I., Tutelea, L. N., Xu, W., & Pucci, M. (2017). Linear electric machines, drives, and MAGLEVs: An overview. *IEEE Transactions on Industrial Electronics*, *65*(9), 7504-7515. doi:10.1109/TIE.2017.2733492.

5. Shahid, M. B., Jin, W., Abbasi, M. A., Husain, A. R. B., Munir, H. M., Hassan, M., ... & Alghamdi, T. A. (2024). Model predictive control for energy efficient AC motor drives: An overview. *IET Electric Power Applications, 18(12), 1894-1920. https://doi.org/10.1049/elp2.12517.*

6. Boldea, I. (2017). Electric generators and motors: An overview. CES Transactions on Electrical Machines and Systems, 1(1), 3-14. doi:10.23919/TEMS.2017.7911104.

7. Gieras, J. F., Piech, Z. J., & Tomczuk, B. (2018). Linear synchronous motors: Transportation and automation systems. CRC Press. https://doi.org/10.3390/en14092549.

8. Jang, S. M., Choi, J. Y., Cho, H. W., & Lee, S. H. (2005). Thrust analysis and measurements of tubular linear actuator with cylindrical halbach array. IEEE Transactions on Magnetics, 41(5), 2028-2031. doi:10.1109/TMAG.2005.846266.

9. Abdalla, I. I., Ibrahim, T., & Nor, N. M. (2018). Analysis of tubular linear motors for different shapes of magnets. IEEE Access, 6, 10297-10310. doi:10.1109/ACCESS.2017.2775863.

10. Bianchi, N., Bolognani, S., Corte, D. D., & Tonel, F. (2003). Tubular linear permanent magnet motors: An overall comparison. IEEE Transactions on Industry Applications, 39(2), 466-475. doi:10.1109/TIA.2003.809444.

11. Leandro, M., Bianchi, N., Molinas, M., & Ummaneni, R. B. (2019, May). Low inductance effects on electric drives using slotless permanent magnet motors: A framework for performance analysis. in IEEE International Electric Machines & Drives Conference (IEMDC), pp. 1099-1105. IEEE. doi:10.1109/IEMDC.2019.8785241.

12. Kang, G., & Nam, K. (2005). Field-oriented control scheme for linear induction motor with the end effect. IEEE Proceedings-Electric Power Applications, 152(6), 1565-1572. https://doi.org/10.1049/ip-epa:20045185.

13. Cui, L., Zhang, H., & Jiang, D. (2019). Research on high efficiency V/f control of segment winding permanent magnet linear synchronous motor. IEEE Access, 7, 138904-138914. doi:10.1109/ACCESS.2019.2930047.

14. Atencia, J., Martinez-Iturralde, M., Martinez, G., Rico, A. G., & Florez, J. (2003, June). Control strategies for positioning of linear induction motor: tests and discussion. in *IEEE International Electric Machines and Drives Conference, 3*, pp. 1651-1655. IEEE. doi:10.1109/IEMDC.2003.1210673.

15. Yu, L., Huang, J., Luo, W., Chang, S., Sun, H., & Tian, H. (2023). Sliding-mode control for PMLSM position control—A review. *Actuators 12*, 31. https://doi.org/10.3390/act12010031.

16. Shao, K., Zheng, J., Wang, H., Wang, X., Lu, R., & Man, Z. (2021). Tracking control of a linear motor positioner based on barrier function adaptive sliding mode. *IEEE Transactions on Industrial Informatics*, *17*(11), 7479-7488. doi:10.1109/TII.2021.3057832.

17. Liu, X., Wu, Q., Zhen, S., Zhao, H., Li, C., & Chen, Y. H. (2022). Robust constraint-following control for permanent magnet linear motor with optimal design: A fuzzy approach. *Information Sciences*, *600*, 362-376. https://doi.org/10.1016/j.ins.2022.03.083.

18. Luo, M., Duan, J. A., & Yi, Z. (2023). Speed tracking performance for a coreless linear motor servo system based on a fitted adaptive fuzzy controller. *Energies*, *16*(3), 1259. https://doi.org/10.3390/en16031259.

19. Liu, Z., Gao, H., Yu, X., Lin, W., Qiu, J., Rodríguez-Andina, J. J., & Qu, D. (2023). B-spline wavelet neural-network-based adaptive control for linear-motor-driven systems via a novel gradient descent algorithm. *IEEE Transactions on Industrial Electronics*, *71*(2), 1896-1905. doi:10.1109/TIE.2023.3260318.

20. Wang, Z., Hu, C., Zhu, Y., He, S., Yang, K., & Zhang, M. (2017). Neural network learning adaptive robust control of an industrial linear motor-driven stage with disturbance rejection ability. *IEEE Transactions on Industrial Informatics*, *13*(5), 2172-2183. doi:10.1109/TII.2017.2684820.

21. Ding, R., Ding, C., Xu, Y., & Yang, X. (2022). Neural-network-based adaptive robust precision motion control of linear motors with asymptotic tracking performance. *Nonlinear Dynamics*, *108*(2), 1339-1356. https://doi.org/10.1007/s11071-022-07258-0.

22. Cheema, M. A. M., & Fletcher, J. E. (2020). *Advanced direct thrust force control of linear permanent magnet synchronous motor*. Springer International Publishing. https://doi.org/10.1007/978-3-030-40325-6.